Received: 18 May 2023 | Accepted: 13 November 2023

DOI: 10.1111/2041-210X.14268

Methods in Ecology and Evolution

RESEARCH ARTICLE

A computational neuroscience framework for quantifying warning signals

O. Penacchio[1,2] | C. G. Halpin[3] | I. C. Cuthill[4] | P. G. Lovell[5] | M. Wheelwright[3] | J. Skelhorn[3] | C. Rowe[3] | J. M. Harris[1]

[1]School of Psychology and Neuroscience, University of St Andrews, St Andrews, Fife, UK

[2]Computer Science Department, Computer Vision Center, Universitat Autònoma de Barcelona, Barcelona, Spain

[3]Centre for Behaviour and Evolution, Newcastle University Biosciences Institute, Newcastle University, Newcastle upon Tyne, UK

[4]School of Biological Sciences, University of Bristol, Bristol, UK

[5]Division of Psychology and Forensic Sciences, School of Applied Sciences, Abertay University, Dundee, UK

Correspondence
O. Penacchio
Email: op5@st-andrews.ac.uk

Funding information
Biotechnology and Biological Sciences Research Council, Grant/Award Number: BB/N005945/1, BB/N00602X/1, BB/N006569/1 and BB/N007239/1; NextGeneration EU (ALRC)

Handling Editor: Graziella Iossa

Abstract

1. Animal warning signals show remarkable diversity, yet subjectively appear to share certain visual features that make defended prey stand out and look different from more cryptic palatable species. For example, many (but far from all) warning signals involve high contrast elements, such as stripes and spots, and often involve the colours yellow and red. How exactly do aposematic species differ from non-aposematic ones in the eyes (and brains) of their predators?
2. Here, we develop a novel computational modelling approach, to quantify prey warning signals and establish what visual features they share. First, we develop a model visual system, made of artificial neurons with realistic receptive fields, to provide a quantitative estimate of the neural activity in the first stages of the visual system of a predator in response to a pattern. The system can be tailored to specific species. Second, we build a novel model that defines a 'neural signature', comprising quantitative metrics that measure the strength of stimulation of the population of neurons in response to patterns. This framework allows us to test how individual patterns stimulate the model predator visual system.
3. For the predator–prey system of birds foraging on lepidopteran prey, we compared the strength of stimulation of a modelled avian visual system in response to a novel database of hyperspectral images of aposematic and undefended butterflies and moths. Warning signals generate significantly stronger activity in the model visual system, setting them apart from the patterns of undefended species. The activity was also very different from that seen in response to natural scenes. Therefore, to their predators, lepidopteran warning patterns are distinct from their non-defended counterparts and stand out against a range of natural backgrounds.
4. For the first time, we present an objective and quantitative definition of warning signals based on how the pattern generates population activity in a neural model of the brain of the receiver. This opens new perspectives for understanding and

J. Skelhorn, C. Rowe and J. M. Harris jointly supervised this work.

testing how warning signals have evolved, and, more generally, how sensory systems constrain signal design.

KEYWORDS
animal pattern, aposematism, avian vision, camouflage, computational neuroscience, defensive coloration, image statistics, Lepidoptera

1 | INTRODUCTION

Aposematic prey have striking colour patterns that warn potential predators that they are unpleasant or unprofitable to eat (Cott, 1940; Mappes et al., 2005; Poulton, 1890; Rowe & Halpin, 2013; Wallace, 1867). Although diverse in nature (Briolat et al., 2019), some common visual characteristics, such as being yellow or red, or having 'high contrast internal boundaries' or 'repetitive elements', are commonly observed in the patterns of aposematic prey and are often considered to be key features that help to deter predators (Guilford & Dawkins, 1993; Mappes et al., 2005; Poulton, 1890; Stevens & Ruxton, 2012). Despite aposematism being a textbook example of adaptation and a key testbed for evolutionary theory (Cuthill et al., 2017; Mappes et al., 2005; Stevens & Ruxton, 2012), we lack an objective quantification of the common visual characteristic of these signals and rely on subjective descriptions of what typifies them.

Existing visual models developed to understand aposematic patterns focus on quantifying how conspicuous a pattern is against the background on which it is found. For example, studies typically use either mathematical properties of the pattern and the background, or model how neurons in visual areas encode these two elements (Barnett, Cuthill, et al., 2018; Barnett, Michalis, et al., 2018; Pike, 2018). While providing valuable insights into how aposematic prey appear against their backgrounds and particularly how conspicuous they might be to a foraging predator, these approaches have not tackled the question of whether aposematic patterns share common properties, or asked what those might be. Here, we take a different approach and apply computational models to compare the patterns of aposematic prey with those of palatable species. We significantly expand on previous spatiochromatic models by developing a two-part modelling framework, based on (1) the responses of classes of artificial neurons that process luminance, pattern and colour information (as others have done, e.g. Pike, 2018), and (2) the response of a novel population model emulating the neural network underlying predator vision. The latter step is important as it allows us to consider each pattern as a coherent whole, rather than breaking it down into notional constituent parts. We apply this computational approach to a novel database of lepidopteran colour patterns where the palatability of each species is known. We show that the diverse warning signals of aposematic prey produce specific neural signatures in the modelled visual systems of their predators that are stronger and distinct from the patterns of more palatable species. We also show that these responses are distinct from the model responses to natural backgrounds.

Our novel framework can quantify and define warning signals based on how the signals themselves are likely to stimulate early sensory systems independent of the backgrounds on which they are found. Our model also offers a predictive tool to test whether any specific prey is likely to be aposematic, based on its pattern, and suggests that it could be the strong neural responses elicited across a population of neurons that underpin predator responses to aposematic prey.

2 | METHODS

2.1 | Model part 1: Computational modelling of visual processing in the predator brain

We focussed on how the colour patterns of Lepidoptera stimulate the visual systems of birds. Birds predating Lepidoptera is a well-established and widely used model system for the study of defensive strategies, particularly aposematism and crypsis (e.g. Cuthill et al., 2005; Kapan, 2001; Ronka et al., 2020), Importantly, the palatability of Lepidoptera to their predators can be extracted from the literature (e.g. Chai, 1986; Pinheiro, 1996), and the visual system of the predator is also relatively well understood (Lind & Kelber, 2011; Olsson et al., 2015, 2016; Osorio et al., 1999). We defined a model to emulate avian vision, based on what we know about their photoreceptors and the first stages of their visual pathway (note, the same approach could be translated to other species of predator using available knowledge of their visual system, or even to other sensory modalities). Here, we used the best characterised model of avian vision, that of the domestic fowl (*Gallus gallus domesticus*) (Olsson et al., 2015, 2016; Osorio et al., 1999; Wilby et al., 2015).

Since colour and luminance are processed in distinct pathways, we separately estimated the response to the patterns of double cones, thought to underlie luminance perception in birds (Bhagavatula et al., 2009; Lind et al., 2014; Osorio et al., 1999) (Model Part 1a, Figure 1c); and responses that underlie colour perception: the four classes of single cone photoreceptors, respectively, sensitive to ultraviolet (U), short (S), medium (M) and long (L) wavelength (Cuthill, 2006; Hart, 2001) (Model Part 1b, Figure 1f). For the achromatic pathway, scans were converted to an avian analogue of luminance using the absorption curve of double cones found in domestic fowl (*Gallus gallus*

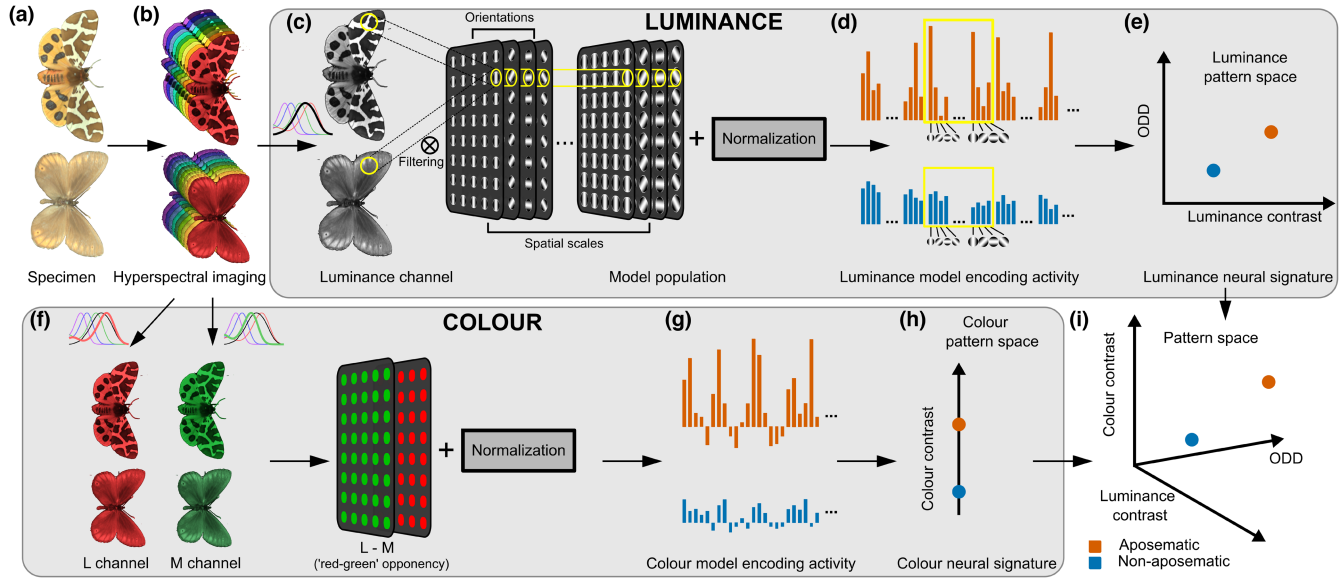

FIGURE 1 (a) A set of aposematic (top, specimen shown, *Arctia caja*, dorsum) and non-aposematic species (bottom, *Oeneis jutta*, dorsum) was identified (referred to as AP and non-AP respectively). (b) Specimens scanned (hyperspectral imaging system, 350–800 nm). (c) Model Part 1a: Luminance pathway. Black boxes illustrate receptive fields of a population of units, each with specific location, orientation and spatial scale. (d) Model Part 2a: Histograms illustrate vector representing activity at each location, orientation and spatial scale, for example, the yellow-boxed region in c delivers higher response at vertical orientation for AP than non-AP patterns (see yellow boxed areas, orange = AP, blue = non-AP). (e) Two summary statistics: *x*-axis, 'luminance contrast', and *y*-axis, Orientation Distribution Deviation, 'ODD'. (f) Model Part 1b: Modelled colour pathway (only the channel contributing to the final colour metric—the 'red-green' channel—is represented). Scans converted to colour response using cone absorption curves of *Gallus gallus domesticus*. Black boxes illustrate a regularly distributed grid of 'red-green' opponent neurons. (g) Model Part 2b: Histograms illustrate vector representing activity in at each location for each orientation and spatial scale. The AP pattern delivers a more varying response (top) than the non-AP pattern (bottom). (h) Output is a single summary statistic, 'colour contrast'. (i) Final output: each sample represented as a location in three-dimensional pattern space.

domesticus). For the colour pathway, scans were converted to colour response using cone absorption curves of the domestic fowl.

2.1.1 | Model part 1a: Luminance pathway

We used current knowledge of the neurobiological architecture that underlies luminance perception in birds. A key concept in biological vision is that of the receptive field. This is defined as a region of space where a sensory stimulus evokes a physiological response. In many taxa, including mammals and birds, pattern vision is achieved through the visual field being sampled by neurons with receptive fields that respond to particular scales of pattern and particular orientations (DeAngelis & Anzai, 2004; Engelage & Bischof, 1996; Hubel & Wiesel, 1962). We emulated that here. The luminance model consisted of units that encode luminance edges at specific topographical locations, for different orientations and spatial scales (coarse to fine), through oriented receptive fields of different orientations and size (see Supplementary Methods 2; Figure S1; Figure 1c (left)). Our model was based on neurons found in the initial processing stages of the visual system of mammals starting with the retina (Devalois et al., 1982; Hubel & Wiesel, 1962), which are also thought to be analogous to neurons found in the avian visual system (Engelage & Bischof, 1996; Li et al., 2007; Pinto & Baron, 2009). This stage of the model comprised a population of units regularly distributed on a spatial ('retinotopic') grid and sensitive to edges with a given orientation and spatial scale (4 orientations and 2 scales shown in Figure 1c, see Supplementary Methods 2 for specific implementation details). The response of the model was computed by considering processing of the luminance images by this population of artificial neurons, followed by a process of nonlinear normalisation of each unit response by the response of neighbouring units. This assumes that the linear responses of each model neuron are modulated by the responses of surrounding neurons following a standard nonlinear centre-surround operation (Stoddard & Osorio, 2019). This operation, called 'divisive normalisation', is found extensively across sensory systems and increases the sensitivity to salient features (Carandini & Heeger, 2012; Itti & Koch, 2001) (Figure 1c). The output of the luminance model was a vector representing activity at each location for each orientation and spatial scale, in response to each pattern. This is visualised in Figure 1d as histograms of activity for each orientation, where each block represents a particular scale. As an example, the yellow-boxed region in Figure 1d delivers higher response at vertical orientation for AP than non-AP patterns (see yellow-boxed areas, orange = AP, blue = non-AP).

2.1.2 | Model part 1b: Colour pathway

To explore the variation in colour (Model Part 1b), we drew on evidence that birds are sensitive to chromatic information encoded by opponent channels, and therefore have a neural correlate for this

information (Goldsmith & Butler, 2005; Osorio et al., 1999). We considered a regularly distributed grid of opponent neurons with a standard colour normalisation (Osorio et al., 1999, Figure 1f). We converted the responses of the simple cones into opponent channel information by considering the L-M ('red-green'), (L+M)-S ('yellow-blue') and U-S ('ultraviolet-blue') channels. These three channels capture the chromatic information available (Osorio et al., 1999). Since the detailed form of the receptive fields underlying colour opponency in birds is not yet identified (Kelber, 2019), we used information from other taxa for which the receptive fields are known (Johnson et al., 2008). We specifically selected the L-M channel for our colour analysis, as variation across the L-M and the (L+M)-S channels was highly correlated for the samples in our database and the response of the U-S channel was similar for the patterns of aposematic and non-aposematic prey (see Supplementary Methods 1) (Figure 1f). This means that the main differences between aposematic and non-aposematic patterns in terms of colour were along what are commonly known as the red–green and yellow–blue axes in colour space, not the ultraviolet–blue axis.

To allow the full range of visible wavelengths to be considered, we exposed the model to a set of hyperspectral images of Lepidoptera (spectral range 350–800 nm, see Section 2.3 below). The output of the colour model was a vector of encoding activity in response to each pattern (as per Figure 1d, representing response at each location for each orientation and spatial scale). In the example shown in Figure 1d, the AP pattern delivers a more varying response (top) than the non-AP pattern (bottom).

2.1.3 | Model part 1: Output across luminance and colour pathways

The output of Part 1 of our model provided two vectors of population activity for each image. These capture activity at each location, orientation and spatial frequency, emulating how luminance and colour are neurobiologically encoded during the initial processing stages of the visual system (Figure 1d,g). A strength of our approach is that straightforward changes to Part 1 of the model allow adaptation to any chosen predator species for which we know the basics of early luminance and colour processing, for example, for bird species with different sensitivities for the L or M cones. Model Part 2 did not retain information on the (L+M)-S and U-S channels (see below) as most of the chromatic information from our Lepidoptera database is at longer wavelengths. Those channels are maintained in Model Part 1 as they are likely to be important when applying the framework in other contexts such as sexual selection. In this case, it would be straightforward to alter the input to the U-S channel for a bird species with a cone type with sensitivity further into the ultraviolet (U type) and matched changes in S cone sensitivity, such as a passerine (Cuthill, 2006; Odeen & Hastad, 2013). The goal of this paper is primarily to showcase the method rather than investigate differences due to predator visual systems; hence, we show modelling based on the domestic fowl only.

2.2 | Model part 2: Metrics of modelled neural activity

The novel part of our modelling approach was to consider the effect of a prey pattern on the whole population of artificial neurons. To obtain a measure of how the population of artificial neurons are stimulated by a single pattern, we defined metrics that summarise the activity of the whole population. Specifically, we defined three summary statistics to characterise modelled brain activity, which we refer to as a 'neural signature' (for the full range of statistics considered, see Supplementary Methods 1). For luminance, we computed the 'luminance contrast' of the patterns using the standard deviation of the luminance population activity, a metric that is a robust correlate of brain activity (Kay et al., 2013; Watson et al., 1983).

Natural scenes have a consistent distribution of contrast across orientations, and deviation with respect to this distribution is important in scene perception and in object categorisation (Girshick et al., 2011; Torralba & Oliva, 2003). With that in mind, we defined a new metric, 'orientation distribution deviation' (ODD), that provides a measure of how the distribution of signal across orientations deviates from that statistically found in natural scenes (an illustration of the two metrics calculated for an AP sample and a non-AP sample is shown in Figure 1e). Our ODD measure considers how the evenness of the distribution of edge orientations at each location on a pattern compares to the typical evenness of the distribution found in natural images. Our baseline was an estimate of the evenness of the distribution of orientations in natural scenes. This estimate was obtained by calculating probability distributions from the histograms of oriented edge energy across orientations for image patches from a large set (more than 1000) of natural images (van Hateren & van der Schaaf, 1998) and at each location on these images, and then computing their 'evenness' as the Shannon entropy of the resulting probability distributions (Cover & Thomas, 2006). The baseline Shannon entropy was computed as the grand average of all the evenness values (2.5 for the model with eight orientations). The ODD is then calculated for each pattern as the standard deviation of the vector of the differences between the Shannon entropy for that pattern at each location and the estimate for natural scenes in general (see Supplementary Methods 3 for details). For example, a stripey pattern will have high ODD because it will contain a peak in the probability distribution for the orientation of the stripes and will have much lower probability at all other orientations.

For colour, we computed the 'colour contrast', defined as the standard deviation of the L-M channel, akin to the computation of 'luminance contrast' (an illustration for the AP and non-AP samples is shown in Figure 1h) (Chaparro et al., 1993).

Overall, these analyses delivered three numbers for each pattern, forming a neural signature that can be plotted in a three-dimensional (3D) 'pattern space' (Stoddard & Osorio, 2019) (Figure 1i shows an illustrative example for the AP and non-AP samples shown in Figure 1a). Thus, the mathematically defined 'neural signature' can

be thought of as a location in a 3D space that defines the whole animal pattern. For all metrics, we combined dorsal and ventral patterns because we wanted to consider each pattern as a coherent whole (see Supplementary Methods 3 for details).

Compared with other mathematical measures of contrast based on adjacent pixel values, for example root-mean-square (RMS) or Michelson contrast (Aronsson & Gamberale-Stille, 2009; Halpin et al., 2020; Prudic et al., 2007), our neural signature captures the spatial structure and arrangement of patterns. To illustrate this, we manipulated the spatial structure of a lepidopteran prey. We randomly scrambled an increasing number of pixels from a pattern, starting with zero percent scrambling (original pattern) to 100% scrambling (all the pixels randomly moved, Figure 2a). This increasingly removed the spatial content of each pattern while retaining luminance and colour content at the pixel level. The luminance contrast and ODD of our model activity progressively decreased (Figure 2b, luminance contrast signature shown in green, ODD in blue). Figure 2c shows that measures of contrast such as the RMS or the Michelson contrast are insensitive to the amount of random scrambling, since they are solely based on pixel information and do not use information about the relative location of the pixels. Therefore, considering models that use receptive-field like structures (Part 1) is essential for effectively discriminating between patterns (see Figure S1 for more details).

2.3 | A database of lepidopteran patterns

To apply the proposed framework, we built a novel database of lepidopteran patterns of aposematic (AP) and non-aposematic (non-AP) species. To build our database, we first searched Google Scholar from 1980 onwards using the term 'aposem*'. From the studies returned, we identified aposematic lepidopteran species and selected them for our study where evidence was consistent with them being defended (e.g. being rejected by predators, or containing known toxins). We then searched for 'palatable' species from the same families for a representative sample of palatable non-aposematic species (any Batesian mimics of aposematic species identified in the literature search were excluded). Again, we checked the literature for evidence of palatability for each species used. The representative set consists of 125 species of Lepidoptera across 12 families for our analysis (96 aposematic and 29 non-aposematic species, see Supplementary Material for

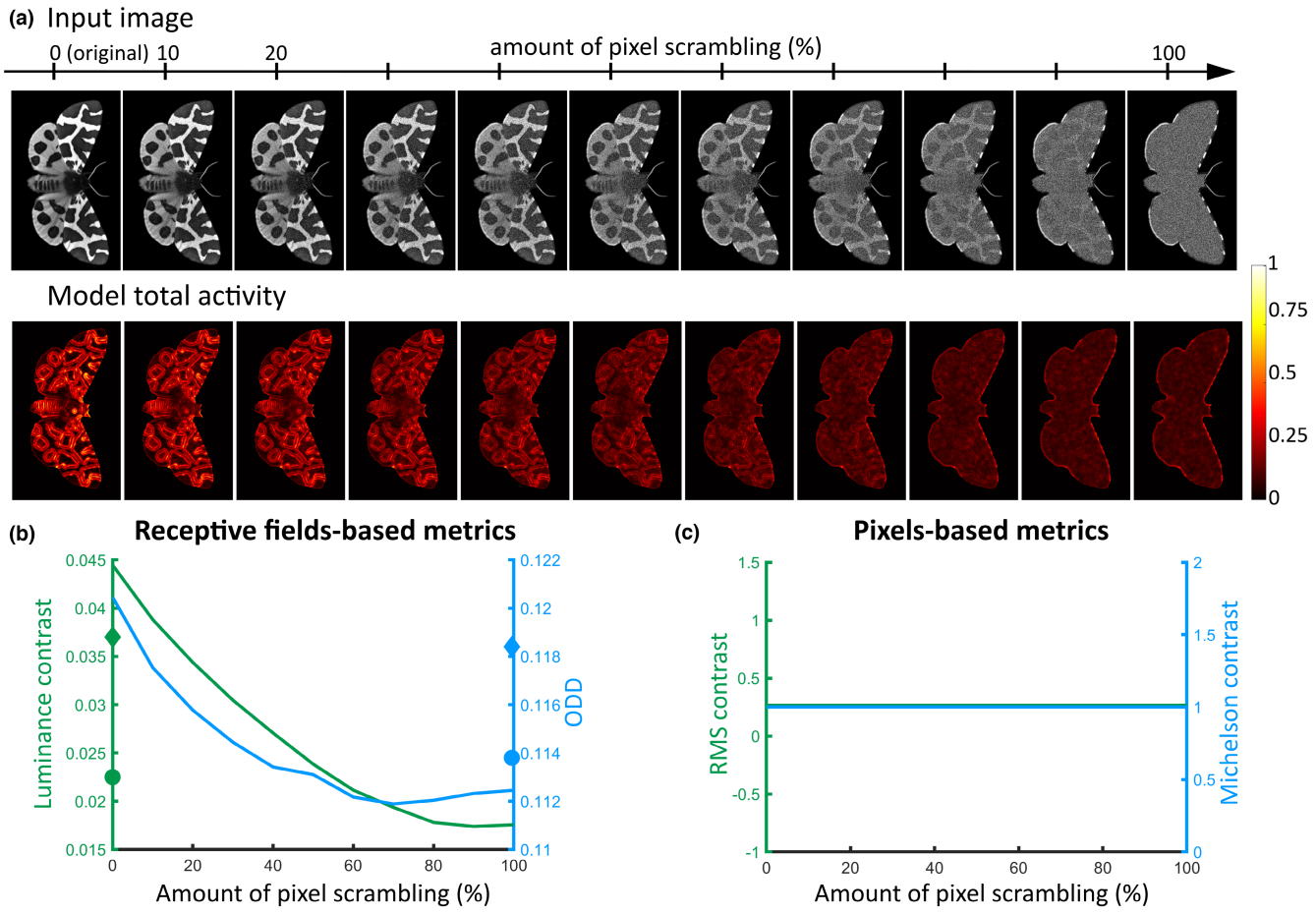

FIGURE 2 (a) (Top row) Random scrambling of an example image (*Arctia caja*, dorsum), from 0% (top left, original image) to 100% (top right, random permutation of all pixels in the pattern) and (bottom row) luminance model total activity (i.e. summed over all orientations and scales) in response to the patterns at the top. (b) Luminance neural signatures against amount of scrambling. (c) Pixel-based metrics of contrast against amount of scrambling (root-mean-square and Michelson contrast lines are overlain).

details). Samples of each species were located in museum collections (the Natural History Museum (BMNH), London, UK; the Manchester Museum (MMUE), Manchester, UK; and the American National Museum (AMNH), New York, USA), and their dorsal and ventral sides were photographed using a hyperspectral camera (Figure 1a,b). In total, we photographed the dorsal and ventral sides of 331 specimens (AP, $N = 244$, average number of specimens per species 5.1, std 2.9; non-AP, $N = 87$, average 6, std 2.8) from the selected species, giving a total of 676 hyperspectral images. Full details on how the list of species was developed and hyperspectral image acquisition are available in Supplementary Information and Supplementary Methods 1. A sample of the database is shown in Figure 3. The database is freely accessible at https://arts.st-andrews.ac.uk/lepidoptera/index.html.

2.4 | Statistical analysis

To test our main hypothesis of the discriminability of AP and non-AP patterns in our modelled neural stimulation space, we ran linear mixed models with pattern category (AP/non-AP) as the independent variable. As predicting pattern membership has potential applications, we also provide the output of logistic regressions, with odds ratios to measure effect size. For this predictive exercise, it should be noted, however, that there are other drivers of colour pattern (e.g. sexual selection), and palatability is still important for confirming anti-predator strategy.

3 | RESULTS

3.1 | Aposematic and non-aposematic patterns elicited different neural activity

3.1.1 | Luminance contrast and ODD

Pattern categories were discriminable by the metrics. The patterns of unpalatable aposematic prey had more luminance contrast (Figure 4a, left panel; linear mixed models with species category as predictor, see Supplementary Method 4 for details on statistical analysis: $\chi^2 = 26.9$, df = 1, $p = 2.12 \times 10^{-7}$, $\Delta AIC = -2484.4 + 2459.5 = -24.9$) and higher ODD (Figure 4a, middle panel, $\chi^2 = 30.4$, df = 1, $p = 3.59 \times 10^{-8}$, $\Delta AIC = -3158 + 3129.7 = -28.3$) than palatable non-aposematic prey. Conversely, luminance contrast and ODD were good predictors of pattern category (logistic regression, with metrics as predictor; luminance contrast: $\chi^2 = 49.32$, df = 1, $p = 2.18 \times 10^{-12}$, $\Delta AIC = 90.1 - 137.4 = -47.3$; ODD: $\chi^2 = 50.28$, df = 1, $p = 1.33 \times 10^{-12}$, $\Delta AIC = 89.1 - 137.4 = -48.3$), with odds ratios of 9.67, 95% confidence interval (CI) = [4.02, 23.27], Wald's test, $p < 0.001$, for luminance contrast, and 10.22, CI = [4.11, 25.39], $p < 0.001$ for ODD. Although these two summary statistics were correlated (Spearman-rank $r = 0.59$, CI = [0.47, 0.70]), the predictive power of a model including both luminance contrast and ODD (Figure 4a, right panel) was better than that of a model including luminance contrast ($\chi^2 = 15.47$, df = 1, $p = 8.36 \times 10^{-5}$, $\Delta AIC = 76.6 - 90.1 = -13.5$) or ODD alone ($\chi^2 = 14.52$, df = 1, $p = 1.39 \times 10^{-4}$, $\Delta AIC = 76.6 - 89.1 = -12.5$). Plotted in a two-dimensional pattern space, aposematic and non-aposematic species therefore tended to occupy different regions (Figure 4b). The way that samples populate the pattern space in Figure 4b illustrates an overall higher luminance contrast and ODD for the warning signals involved in AP patterns (orange dots) compared to the non-AP species (blue dots). The background colour corresponds to predicted pattern category (pale orange, AP species; pale blue, non-AP) according to the binary classification provided by a logistic regression of pattern category on luminance contrast and ODD for the full luminance pattern space (see Section 2).

3.1.2 | Colour contrast

Figure 5a (left panel) illustrates the spread of colour contrast across the patterns. Each panel show the distribution of one of these measures for AP species (orange, $N = 96$) and non-AP species (blue, $N = 29$). Each dot represents the average over all specimens and sides (dorsal and ventral) for one of the 125 species in the database. Colour contrast discriminated the two categories, with higher values in aposematic than non-aposematic prey ($\chi^2 = 10.3$, df = 1, $p = 0.0013$, $\Delta AIC = -1804.7 + 1796.3 = -8.4$). Conversely, colour contrast was a good predictor of pattern category ($\chi^2 = 33.97$, df = 1, $p = 5.59 \times 10^{-9}$, $\Delta AIC = 105.4 - 137.4 = -32$; odds ratios of 8.67, 95% confidence interval CI = [3.4, 22.1], Wald's test, $p < 0.001$).

3.1.3 | Combination of luminance metrics and colour

Combining colour and luminance metrics better discriminates between aposematic and non-aposematic patterns than either dimension alone. Figure 5c shows scatterplot of the three metrics, with background colour corresponding to predicted pattern category (orange, AP species; pale blue, non-AP species) according to the binary classification provided by a logistic regression of pattern category on luminance contrast, ODD and colour contrast for the full three-dimensional pattern space. The predictive power of this statistical model, combining colour contrast with the two luminance summary statistics, was higher than that of a simpler model including only the two luminance summary statistics ($\chi^2 = 5.66$, df = 1, $p = 0.0174$, $\Delta AIC = 73.0 - 76.4 = -3.4$) or the colour summary statistics only ($\chi^2 = 36.48$, df = 1, $p = 1.20 \times 10^{-8}$, $\Delta AIC = 73 - 105.5 = -32.5$). We also visualised luminance contrast, ODD and colour contrast in a three-dimensional pattern space (Figure 5c). The space can be separated into two regions (shown

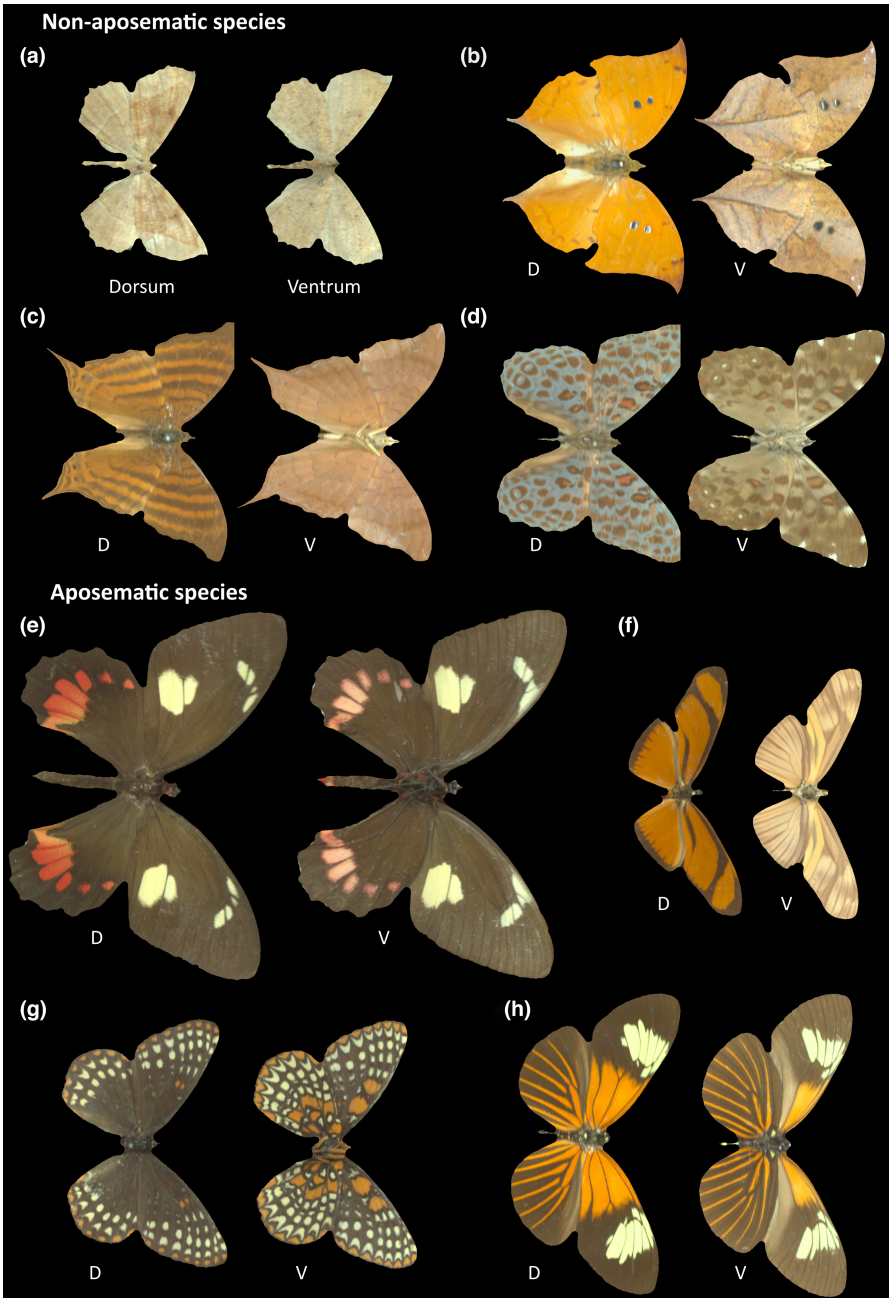

FIGURE 3 Non-aposematic (a–d) and aposematic (e–h) samples of the Lepidoptera hyperspectral database. (a) *Eutrapela clemataria*. (b) *Zaretis ellops*. (c) *Marpesia norica*. (d) *Hamadryas chloe*. (e) *Parides childrenae*. (f) *Eueides aliphera*. (g) *Euphydryas phaeton*. (h) *Heliconius xanthocles*. The relative size of the specimens is respected.

by pale blue and orange shading in Figure 5c), with aposematic patterns typically associated with higher values for the three summary statistics compared to non-aposematic patterns. The separation correctly classified 87.2% of the species (evaluated using 10-fold cross-validation, see Supplementary Methods 4). Therefore, taken together, our framework based on avian visual processing provides a clear separation between warning signals and patterns of undefended species. Note that the separation is based on objective differences in a neural stimulation space and does not correspond to 'how similar' the patterns may appear to us. Insets in Figure 5c give an example. The dorsal (D, left side) and ventral (V, right side) colouration of two AP species with adjacent neural signatures is shown (*Diaethria clymena*, left, and *Danaus plexippus*, right). These patterns look very different, but have similar neural signatures.

3.2 | Analyses within Lepidoptera families

If these neural signatures characterise warning signals, we expect to see them replicated at different taxonomic scales. To explore this, we repeated the comparisons of the three metrics above using the five families in our that data set that include both aposematic and non-aposematic species (Erebidae, Geometridae, Nymphalidae, Pieridae and Pyralidae). We used a bootstrapping method to draw pairs randomly (with replacement) to repeatedly resample the maximum number

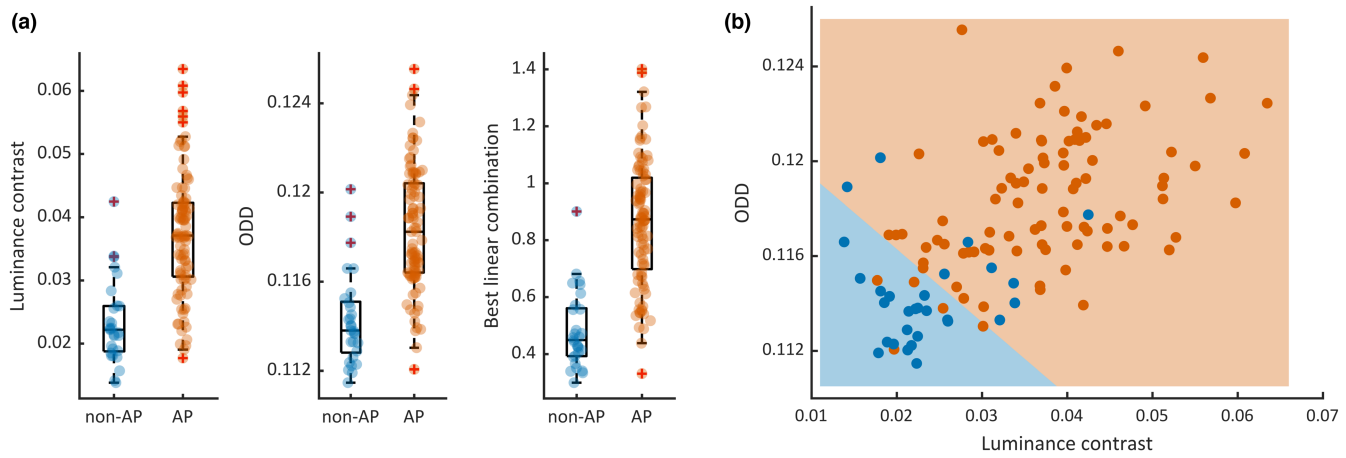

FIGURE 4 (a) Graphs show luminance contrast, Orientation Distribution Deviation (ODD) and the best linear combination between luminance contrast and ODD statistics of the model population activity in response to AP (orange, $N=96$) and non-AP (blue, $N=29$) patterns. Values correspond to the species average across all specimens and both sides (dorsal and ventral). Boxplots show median, the 25th and 75th percentiles (lower and upper hinges), the lowest measured values within Q1 (first quantile) and 1.5 × Q1 (lower whisker) and the highest observed value within Q3 (third quantile) and 1.5 × Q3 (upper whisker). (b) Scatterplot of luminance contrast and ODD as a two-dimensional pattern space. Background colour is predicted pattern category (pale orange, AP species; pale blue, non-AP) from a logistic regression (see Section 2). Each species can be identified in Supplementary Result 2, Figure S4.

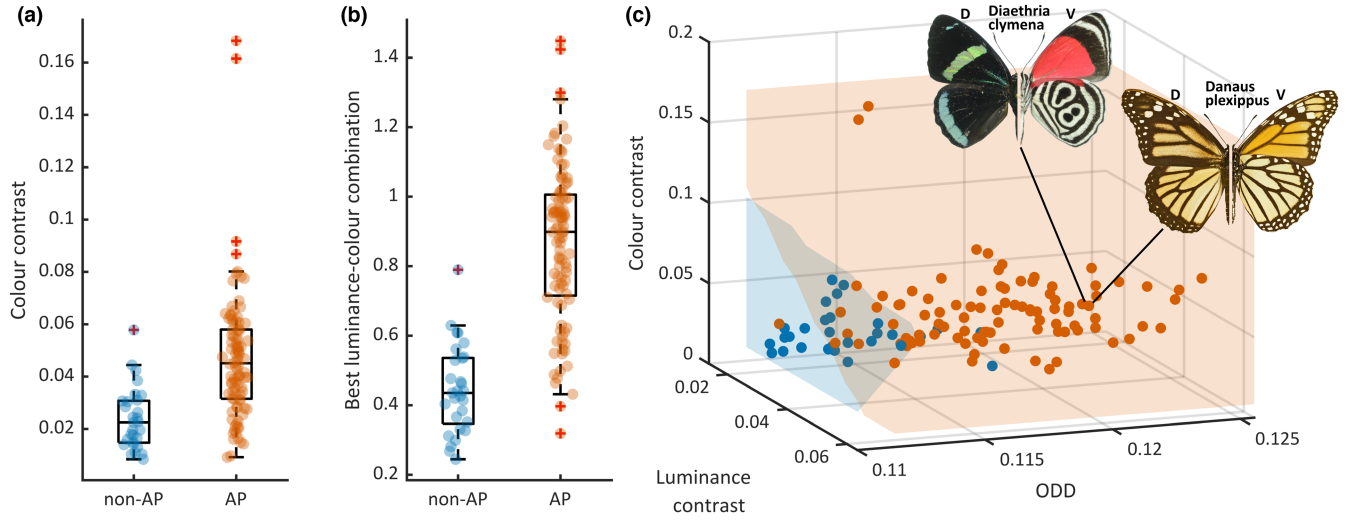

FIGURE 5 (a) Colour contrast and (b) best linear combination between luminance contrast, Orientation Distribution Deviation (ODD) and colour contrast for AP (orange) and non-AP (blue) patterns. (c) Scatterplot of luminance contrast, ODD and colour contrast as a three-dimensional pattern space. Background colour is predicted pattern category (pale orange, AP species; pale blue, non-AP) from a logistic regression (see Section 2). Background colour is predicted pattern category (orange, AP species; pale blue, non-AP species) from a logistic regression. Insets: the dorsal (D, left side) and ventral (V, right side) colouration of two AP species with adjacent neural signatures (*Diaethria clymena*, left, and *Danaus plexippus*, right). Image credit: *D. clymena* dorsal and ventral adapted from Geoff Gallice (CC-BY-2.0); *D. plexippus* adapted from Didier Descouens (CC BY-SA 3.0).

of possible pairs in these families (namely 26) to estimate the summary statistics for the two categories of patterns (see Supplementary Result 3). Consistent with our overall findings, we found that luminance contrast, ODD and colour contrast were generally higher for aposematic than non-aposematic species in the five families (Figure 6, all $p<10^{-6}$ except for ODD in Pieridae, see Supplementary Result 3).

FIGURE 6 (a) Comparison of the luminance contrast; (b) Orientation Distribution Deviation (ODD); and (c) colour contrast summary statistics between AP species (orange dots) and non-AP species (blue dots) within the same family for all families in the database that contained both AP and non-AP species (family, total number of species = number of non-AP species + number of AP species: Erebidae, 13 = 1 + 12; Geometridae, 17 = 9 + 8; Nymphalidae, 61 = 12 + 49; Pieridae, 8 = 4 + 4; Pyralidae, 2 = 1 + 1). All conventions as in Figure 4.

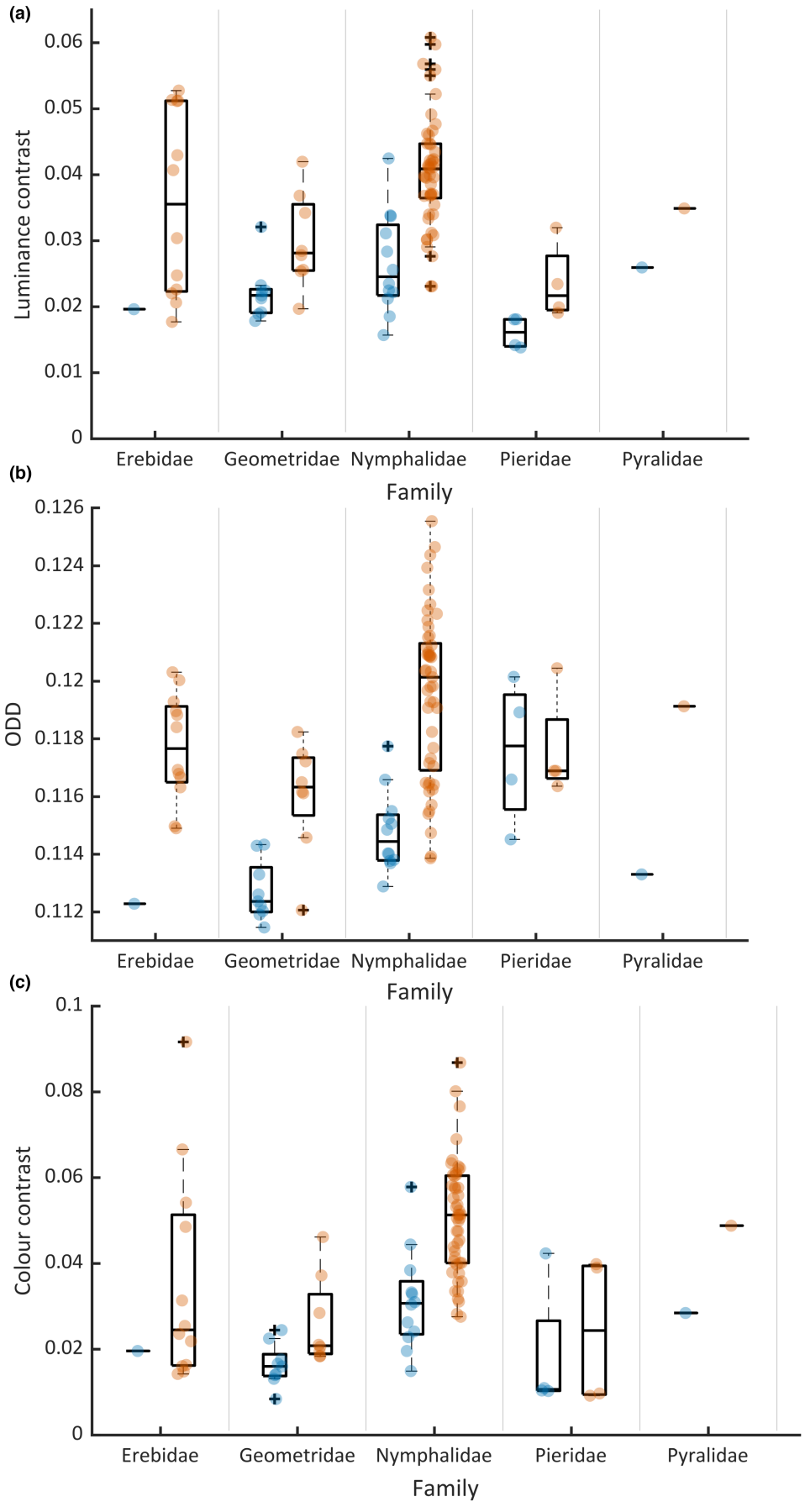
(a)
Luminance contrast
0.06
0.05
0.04
0.03
0.02
0.01
0
Erebidae
Geometridae
Nymphalidae
Pieridae
Pyralidae
Family
(b)
ODD
0.126
0.124
0.122
0.12
0.118
0.116
0.114
0.112
Erebidae
Geometridae
Nymphalidae
Pieridae
Pyralidae
Family
(c)
Colour contrast
0.1
0.08
0.06
0.04
0.02
0
Erebidae
Geometridae
Nymphalidae
Pieridae
Pyralidae
Family

3.3 | Aposematic species stand out in typical natural scenes

Aposematic signals are thought to have been selected to not only enhance predators' abilities to discriminate between palatable and defended prey, but to also increase prey conspicuousness in natural environments and enhance predator avoidance (Stevens & Ruxton, 2012). To test this, we first presented patches of natural scenes to our model to extract their luminance and colour neural signatures. We then compared the differences in frequency distributions of our three summary statistics between natural backgrounds and those for aposematic and non-aposematic prey (Figure 7). Natural backgrounds were obtained by sampling patched from images in the van Hateren database of calibrated natural images (van Hateren & van der Schaaf, 1998) (see Section 2). We found that aposematic patterns had frequency distributions with higher values compared to those of natural backgrounds, for all three summary statistics (luminance contrast, $\bar{z} = 0.55$, Figure 7a; ODD, $\bar{z} = 1.43$, Figure 7b; colour contrast, $\bar{z} = 1.72$, Figure 7c). In contrast, the frequency distributions for non-aposematic prey were a much closer match to those of natural scenes, and even slightly lower in the case of luminance contrast (luminance contrast, $\bar{z} = -0.67$, Figure 7a; ODD, $\bar{z} = 0.04$, Figure 7b, colour contrast, $\bar{z} = 0.21$, Figure 7c). Figure 7d shows a two-dimensional representation of the luminance signatures and illustrates how aposematic patterns (orange dots) are located well away from the centre of the distribution for natural images (yellow region) towards higher values for both signatures. Note that each of the 4096 black dots in Figure 7d corresponds to a single patch in the van Hateren database of calibrated natural images (van Hateren & van der Schaaf, 1998) (see Section 2). These data suggest that aposematic patterns do not simply have colours and patterns that are different from those found in natural scenes but have been selected to deliver a stronger neural signature, and thus be more conspicuous in the natural world.

4 | DISCUSSION

Our novel modelling framework, based on a biologically realistic model of predator vision, provides an objective and quantitative method for discriminating between aposematic and non-aposematic

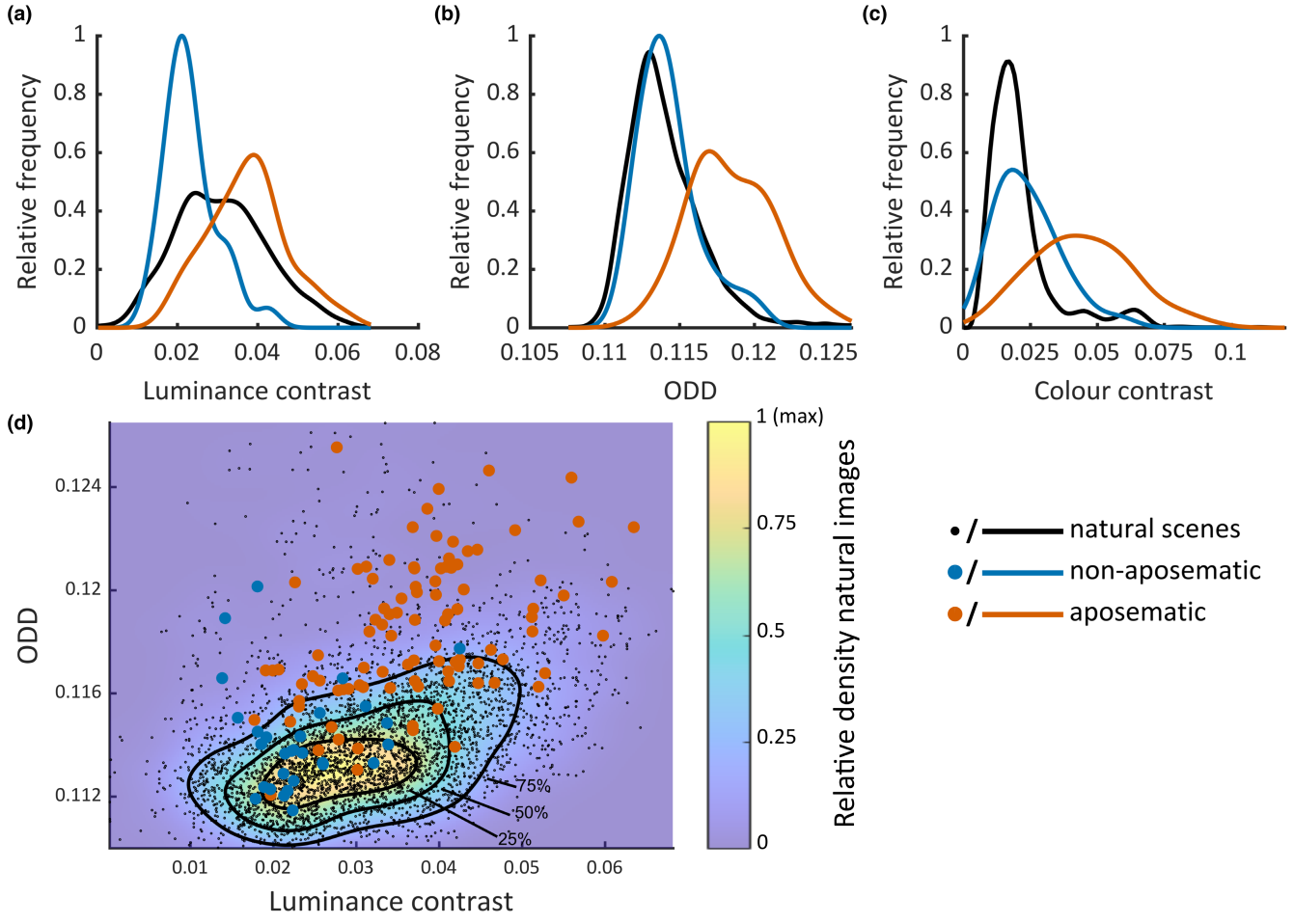

FIGURE 7 Distributions of (a) luminance contrast; (b) Orientation Distribution Deviation (ODD); and (c) colour contrast for (black line) natural images, (blue) non-AP species and (orange) AP species. (d) Distributions of luminance signatures for AP and non-AP species relative to those for natural images (orange dots: AP, blue dots: non-AP, black dots: patches of images from natural image database). Background colours: density of the distribution of values for natural image patches (yellow, higher density; purple, lower density), with black lines showing contour for higher 25th, 50th and 75th percentile.

patterns in Lepidoptera. The framework enables us to define and classify warning signals based on how they stimulate neural responses in our model, without the need for information about the background against which they are viewed. Intriguingly, warning patterns appear to share distinct 'neural signatures' that could make them stand out from palatable prey and a wide variety of natural backgrounds, and potentially make them easier to learn and avoid. Our results provide objective evidence for the (previously subjective) observation that lepidopteran warning signals share the features of high contrast, bold (often long wavelength) colours, and distinctive patterning that differentiates them from both backgrounds and non-aposematic prey. They additionally reveal that there are many ways to be aposematic: patterns and colours that appear very different to the experimenter can be similarly potent aposematic patterns to a model visual system. Importantly, the model framework can be applied to a range of signalling systems in order to generate testable predictions about how selection has shaped signals to be particularly effective against their intended receivers.

In recent years, several modelling approaches to understand animal defensive coloration have integrated biologically realistic elements of predator vision (Pike, 2018; Stevens & Cuthill, 2006; Stoddard et al., 2014; Troscianko et al., 2017; van den Berg et al., 2020). Some work has quantified coloration patterns on a continuum between crypsis and conspicuousness using the response of units sensitive to luminance edges with receptive fields similar to those in our model. For example, modelling with such units has been used to measure how an animal pattern disrupts its outline on a given background, to quantify disruptive colouration (Stevens & Cuthill, 2006; Troscianko et al., 2017). Conspicuousness with respect to a background can be quantified following a generic model of visual attention (Itti & Koch, 2000) by comparing the distribution of responses of similar units between target animal and background (Barnett et al., 2017, 2021; Michalis et al., 2017; Pike, 2018). Our work is different in emphasis as it aims to understand the design of warning signals per se, by characterising how these signals specifically stimulate a detailed model of the visual brain of the receiver, with no reference to a specific background. This allows us to define a 'pattern space' (Stoddard & Osorio, 2019), based on visual processing of evolved colour patterns as a whole rather than a sum of separate components, so that patterns can be compared with one another, across species, as well as against natural backgrounds.

Our approach and findings emphasise that there may be no simple 'recipe' for building a pattern that is strongly aposematic, but instead suggests a general principle: that an aposematic pattern has a specifically strong effect on visual brain areas in predators. In other words, aposematic signals do not have to rely on the presence of specific physical colours or specific physical pattern elements (Aronsson & Gamberale-Stille, 2009; Guilford, 1990; Stevens & Ruxton, 2012), but on the effect, pattern elements have on the brain of the receiver. This can explain the diversity of warning signals (Stevens & Ruxton, 2012), as it means that there are many ways to produce a strong aposematic signal, and suggests that a range of patterns that look very different to us may affect predators in very similar ways (see Figure 4 insets showing two differently patterned species, with similar neural signatures). It also means that there is a risk that some aposematic patterns have been overlooked by researchers, and our work may facilitate the discovery and study of aposematic species with patterns that fall outside what the literature has considered the norm. It also challenges the assumption that warning signals without typical features described in the literature are somehow 'weak' and less effective (Wuster et al., 2004), and instead helps to generate testable predictions about which patterns will be the strongest and most effective (Halpin et al., 2020).

Our results suggest that warning patterns exploit sensory mechanisms through eliciting stronger neural signals in predators' brains. While our results are based on a single predator–prey system, the ways in which visual processing is conserved across taxa would suggest that our finding can be extended to warning signals more generally. Our modelling was based solely on processes that occur before any cognitive processing of the visual information occurs, and for all three metrics we considered, there was greater activity in the modelled brain for the aposematic patterns than the non-aposematic patterns. This suggests a hitherto non-contemplated reason for why warning signals have an effect on predators that provides a clear prediction for future testing: Sensory processing alone could explain why warning signals are easier to learn and remember (Santangelo, 2015).

When comparing animal patterns against a wide range of generic natural backgrounds, we found that the frequency distributions of our three metrics were rather similar for backgrounds and non-aposematic prey (Figure 7); yet there were strikingly different between backgrounds and aposematic prey. This offers a statistical explanation for which patterns might offer camouflage or conspicuousness. Importantly, Figure 7 shows strong evidence that it may be possible for aposematic patterns to systematically differ from most natural backgrounds. Natural scenes, despite their apparent diversity, share consistent regularities, for example, in how contrast varies across spatial scales (Field, 1987). Strong theoretical and empirical evidence shows that visual systems adapt over evolutionary time to these statistical regularities (Atick & Redlich, 1992; Baker & Graf, 2009; Barlow, 1961; Field, 1987; Parraga et al., 2000). Recent evidence suggests that these regularities may play a role in sexually selected traits (Hulse et al., 2020; Renoult et al., 2016). If a pattern departs from the statistical structure of natural scenes by deviating from the way contrast varies across scales, as arrangements of spots and stripes do (Penacchio, Otazu, et al., 2023; Penacchio & Wilkins, 2015), it will differ from most natural backgrounds.

This work also has wider implications for the understanding of visual signalling. Although focussed on how Lepidopteran patterns stimulate a model avian visual system, our approach is based on well-known components of visual systems that are likely to be conserved across a range of species (Kelber et al., 2003; Osorio & Cuthill, 2015), meaning that it could potentially be used to study the patterns of animals across different contexts with a wide variety of receivers. While our model could be refined as we learn more about avian brains, especially the machinery of avian colour vision including its

spatial organisation (Kelber, 2019), the key point is that we have added a novel development to the literature on sensory drive, sensory exploitation and receiver psychology (Endler & Basolo, 1998; Guilford & Dawkins, 1993) by offering an objective and quantitative definition of warning signals grounded in how patterns trigger activity in a model of predators' brain.

AUTHOR CONTRIBUTIONS

Conceptualisation: O. Penacchio, J. M. Harris, C. Rowe, J. Skelhorn and I. C. Cuthill; Data curation: O. Penacchio, C. G. Halpin, C. Rowe and J. M. Harris; Software: O. Penacchio; Formal Analysis: O. Penacchio, J. M. Harris and I. C. Cuthill; Methodology: O. Penacchio, C. G. Halpin, J. M. Harris, C. Rowe, J. Skelhorn, I. C. Cuthill and P. G. Lovell; Investigation: O. Penacchio, C. G. Halpin and M. Wheelwright; Administration, supervision: J. M. Harris, C. Rowe and J. Skelhorn; Visualisation: O. Penacchio; Writing—original draft: O. Penacchio, J. M. Harris, J. Skelhorn and C. Rowe; Writing—review and editing: All authors; Funding: O. Penacchio, J. M. Harris, C. Rowe, J. Skelhorn, I. C. Cuthill and P. G. Lovell.

ACKNOWLEDGEMENTS

We would like to thank Diana Umeton and Grace Holmes for their help with data collection, Geoff Martin (BMNH) for access to specimens and logistical support, Courtney Richenbacher and David Grimaldi (AMNH), and Dmitri Logunov and Phil Rispin (MMUE) for providing us with specimens. We would also like to thank Jolyon Troscianko for discussions that helped improve the manuscript's focus. This work was funded by BBSRC grants awarded to J.M.H. and O.P. (BB/N006569/1), C.R. and J.S. (BB/N00602X/1), P.G.L. (BB/N005945/1) and I.C.C. (BB/N007239/1). O.P. was also funded by a Maria Zambrano Fellowship for attraction of international talent for the requalification of the Spanish university system—NextGeneration EU (ALRC).

CONFLICT OF INTEREST STATEMENT

The authors declare no competing interests.

PEER REVIEW

The peer review history for this article is available at https://www.webofscience.com/api/gateway/wos/peer-review/10.1111/2041-210X.14268.

DATA AVAILABILITY STATEMENT

All the hyperspectral images are available at https://arts.st-andrews.ac.uk/lepidoptera/. The data, Matlab and R code that support the findings of this study—including a full description of the Matlab functions involved in the computational pipeline to compute the metrics—are openly available at Dryad Digital Repository https://doi.org/10.5061/dryad.x3ffbg7kd (Penacchio, Halpin, et al., 2023).

ORCID

O. Penacchio https://orcid.org/0000-0002-1544-2405
I. C. Cuthill https://orcid.org/0000-0002-5007-8856
P. G. Lovell https://orcid.org/0000-0003-2959-5370
J. Skelhorn https://orcid.org/0000-0002-8385-4831
C. Rowe https://orcid.org/0000-0001-5379-843X
J. M. Harris https://orcid.org/0000-0002-3497-4503

REFERENCES

Aronsson, M., & Gamberale-Stille, G. (2009). Importance of internal pattern contrast and contrast against the background in aposematic signals. *Behavioral Ecology*, *20*, 1356–1362.

Atick, J. J., & Redlich, A. N. (1992). What does the retina know about natural scenes. *Neural Computation*, *4*, 196–210.

Baker, D. H., & Graf, E. W. (2009). Natural images dominate in binocular rivalry. *Proceedings of the National Academy of Sciences of the United States of America*, *106*, 5436–5441.

Barlow, H. B. (1961). *Possible principles underlying the transformations of sensory messages. A Symposium*. MIT Press.

Barnett, J. B., Cuthill, I. C., & Scott-Samuel, N. E. (2017). Distance-dependent pattern blending can camouflage salient aposematic signals. *Proceedings of the Royal Society B: Biological Sciences*, *284*, 6.

Barnett, J. B., Cuthill, I. C., & Scott-Samuel, N. E. (2018). Distance-dependent aposematism and camouflage in the cinnabar moth caterpillar (*Tyria jacobaeae*, Erebidae). *Royal Society Open Science*, *5*, 6.

Barnett, J. B., Michalis, C., Scott-Samuel, N. E., & Cuthill, I. C. (2018). Distance-dependent defensive coloration in the poison frog *Dendrobates tinctorius*, Dendrobatidae. *Proceedings of the National Academy of Sciences of the United States of America*, *115*, 6416–6421.

Barnett, J. B., Michalis, C., Scott-Samuel, N. E., & Cuthill, I. C. (2021). Colour pattern variation forms local background matching camouflage in a leaf-mimicking toad. *Journal of Evolutionary Biology*, *34*, 1531–1540.

Bhagavatula, P., Claudianos, C., Ibbotson, M., & Srinivasan, M. (2009). Edge detection in landing budgerigars (*Melopsittacus undulatus*). *PLoS ONE*, *4*, 10.

Briolat, E. S., Burdfield-Steel, E. R., Paul, S. C., Ronka, K. H., Seymoure, B. M., Stankowich, T., & Stuckert, A. M. M. (2019). Diversity in warning coloration: Selective paradox or the norm? *Biological Reviews*, *94*, 388–414.

Carandini, M., & Heeger, D. J. (2012). Normalization as a canonical neural computation. *Nature Reviews Neuroscience*, *13*, 51–62.

Chai, P. (1986). Field observations and feeding experiments on the responses of rufous-tailed jacamars (*Galbula ruficauda*) to free-flying butterflies in a tropical rain-forest. *Biological Journal of the Linnean Society*, *29*, 161–189.

Chaparro, A., Stromeyer, C. F., Huang, E. P., Kronauer, R. E., & Eskew, R. T. (1993). Color is what the eye sees best. *Nature*, *361*, 348–350.

Cott, H. B. (1940). *Adaptive coloration in animals*. Methuen & Co. Ltd.

Cover, T. M., & Thomas, J. A. (2006). *Elements of information theory (Wiley series in telecommunications and signal processing)*. Wiley-Interscience.

Cuthill, I. C. (2006). *Color perception*. Harvard University Press.

Cuthill, I. C., Allen, W. L., Arbuckle, K., Caspers, B., Chaplin, G., Hauber, M. E., Hill, G. E., Jablonski, N. G., Jiggins, C. D., Kelber, A., Mappes, J., Marshall, J., Merrill, R., Osorio, D., Prum, R., Roberts, N. W., Roulin, A., Rowland, H. M., Sherratt, T. N., … Caro, T. (2017). The biology of color. *Science*, *357*(7), eaan0221.

Cuthill, I. C., Stevens, M., Sheppard, J., Maddocks, T., Parraga, C. A., & Troscianko, T. S. (2005). Disruptive coloration and background pattern matching. *Nature*, *434*, 72–74.

DeAngelis, G. C., & Anzai, A. (2004). A modern view of the classical receptive field: Linear and non-linear spatio-temporal processing by V1 neurons. In L. M. Chalupa & J. S. Werner (Eds.), *The visual neurosciences* (pp. 704–719). MIT Press.

Devalois, R. L., Albrecht, D. G., & Thorell, L. G. (1982). Spatial-frequency selectivity of cells in macaque visual-cortex. *Vision Research*, *22*, 545–559.

Endler, J. A., & Basolo, A. L. (1998). Sensory ecology, receiver biases and sexual selection. *Trends in Ecology & Evolution*, *13*, 415–420.

Engelage, J., & Bischof, H. J. (1996). Single cell responses in the ectostriatum of the zebra finch. *Journal of Comparative Physiology A. Neuroethology, Sensory, Neural, and Behavioral Physiology*, *179*, 785–795.

Field, D. J. (1987). Relations between the statistics of natural images and the response properties of cortical cells. *Journal of the Optical Society of America A. Optics, Image Science, and Vision*, *4*, 2379–2394.

Girshick, A. R., Landy, M. S., & Simoncelli, E. P. (2011). Cardinal rules: Visual orientation perception reflects knowledge of environmental statistics. *Nature Neuroscience*, *14*, 926–932.

Goldsmith, T. H., & Butler, B. K. (2005). Color vision of the budgerigar (*Melopsittacus undulatus*): Hue matches, tetrachromacy, and intensity discrimination. *Journal of Comparative Physiology A. Neuroethology, Sensory, Neural, and Behavioral Physiology*, *191*, 933–951.

Guilford, T. (1990). The secrets of aposematism—Unlearned responses to specific colors and patterns. *Trends in Ecology & Evolution*, *5*, 323.

Guilford, T., & Dawkins, M. S. (1993). Receiver psychology and the design of animal signals. *Trends in Neurosciences*, *16*, 430–436.

Halpin, C. G., Penacchio, O., Lovell, P. G., Cuthill, I. C., Harris, J. M., Skelhorn, J., & Rowe, C. (2020). Pattern contrast influences wariness in naive predators towards aposematic patterns. *Scientific Reports*, *10*(8), 9246.

Hart, N. S. (2001). The visual ecology of avian photoreceptors. *Progress in Retinal and Eye Research*, *20*, 675–703.

Hubel, D. H., & Wiesel, T. N. (1962). Receptive fields, binocular interaction and functional architecture in cats visual cortex. *Journal of Physiology (London)*, *160*, 106–154.

Hulse, S. V., Renoult, J. P., & Mendelson, T. C. (2020). Sexual signaling pattern correlates with habitat pattern in visually ornamented fishes. *Nature Communications*, *11*, 8.

Itti, L., & Koch, C. (2000). A saliency-based search mechanism for overt and covert shifts of visual attention. *Vision Research*, *40*, 1489–1506.

Itti, L., & Koch, C. (2001). Computational modelling of visual attention. *Nature Reviews Neuroscience*, *2*, 194–203.

Johnson, E. N., Hawken, M. J., & Shapley, R. (2008). The orientation selectivity of color-responsive neurons in macaque V1. *Journal of Neuroscience*, *28*, 8096–8106.

Kapan, D. D. (2001). Three-butterfly system provides a field test of müllerian mimicry. *Nature*, *409*, 338–340.

Kay, K. N., Winawer, J., Rokem, A., Mezer, A., & Wandell, B. A. (2013). A two-stage cascade model of BOLD responses in human visual cortex. *PLoS Computational Biology*, *9*, e1003079. https://doi.org/10.1371/journal.pcbi.1003079

Kelber, A. (2019). Bird colour vision - from cones to perception. *Current Opinion in Behavioral Sciences*, *30*, 34–40.

Kelber, A., Vorobyev, M., & Osorio, D. (2003). Animal colour vision—Behavioural tests and physiological concepts. *Biological Reviews*, *78*, 81–118.

Li, D. P., Xiao, Q., & Wang, S. R. (2007). Feedforward construction of the receptive field and orientation selectivity of visual neurons in the pigeon. *Cerebral Cortex*, *17*, 885–893.

Lind, O., Chavez, J., & Kelber, A. (2014). The contribution of single and double cones to spectral sensitivity in budgerigars during changing light conditions. *Journal of Comparative Physiology A. Neuroethology, Sensory, Neural, and Behavioral Physiology*, *200*, 197–207.

Lind, O., & Kelber, A. (2011). The spatial tuning of achromatic and chromatic vision in budgerigars. *Journal of Vision*, *11*, 9.

Mappes, J., Marples, N., & Endler, J. A. (2005). The complex business of survival by aposematism. *Trends in Ecology & Evolution*, *20*, 598–603.

Michalis, C., Scott-Samuel, N. E., Gibson, D. P., & Cuthill, I. C. (2017). Optimal background matching camouflage. *Proceedings of the Royal Society B: Biological Sciences*, *284*, 6.

Odeen, A., & Hastad, O. (2013). The phylogenetic distribution of ultraviolet sensitivity in birds. *BMC Evolutionary Biology*, *13*, 10.

Olsson, P., Lind, O., & Kelber, A. (2015). Bird colour vision: Behavioural thresholds reveal receptor noise. *Journal of Experimental Biology*, *218*, 184–193.

Olsson, P., Wilby, D., & Kelber, A. (2016). Quantitative studies of animal colour constancy: Using the chicken as model. *Proceedings of the Royal Society B: Biological Sciences*, *283*, 20160411. https://doi.org/10.1098/rspb.2016.0411

Osorio, D., & Cuthill, I. C. (2015). *Camouflage and perceptual organization in the Animal Kingdom*. Oxford University Press.

Osorio, D., Vorobyev, M., & Jones, C. D. (1999). Colour vision of domestic chicks. *Journal of Experimental Biology*, *202*, 2951–2959.

Parraga, C. A., Troscianko, T., & Tolhurst, D. J. (2000). The human visual system is optimised for processing the spatial information in natural visual images. *Current Biology*, *10*, 35–38.

Penacchio, O., Halpin, C., Cuthill, I. C., Lovell, P. G., Wheelwright, M., Skelhorn, J., Rowe, C., & Harris, J. M. (2023). A computational neuroscience framework for quantifying warning signals [dataset]. *Dryad Digital Repository*, https://doi.org/10.5061/dryad.x3ffbg7kd

Penacchio, O., Otazu, X., Wilkins, A. J., & Haigh, S. M. (2023). A mechanistic account of visual discomfort. *Frontiers in Neuroscience*, *17*, 14.

Penacchio, O., & Wilkins, A. J. (2015). Visual discomfort and the spatial distribution of Fourier energy. *Vision Research*, *108*, 1–7.

Pike, T. W. (2018). Quantifying camouflage and conspicuousness using visual salience. *Methods in Ecology and Evolution*, *9*, 1883–1895.

Pinheiro, C. E. G. (1996). Palatability and escaping ability in neotropical butterflies: Tests with wild kingbirds (*Tyrannus melancholicus*, Tyrannidae). *Biological Journal of the Linnean Society*, *59*, 351–365.

Pinto, L., & Baron, J. (2009). Spatiotemporal frequency and speed tuning in the owl visual wulst. *European Journal of Neuroscience*, *30*, 1251–1268.

Poulton, E. B. (1890). *The Colours of animals: Their meaning and use especially considered in the case of insects*. D. Appleton and Company.

Prudic, K. L., Skemp, A. K., & Papaj, D. R. (2007). Aposematic coloration, luminance contrast, and the benefits of conspicuousness. *Behavioral Ecology*, *18*, 41–46.

Renoult, J. P., Bovet, J., & Raymond, M. (2016). Beauty is in the efficient coding of the beholder. *Royal Society Open Science*, *3*, 8.

Ronka, K., Valkonen, J. K., Nokelainen, O., Rojas, B., Gordon, S., Burdfield-Steel, E., & Mappes, J. (2020). Geographic mosaic of selection by avian predators on hindwing warning colour in a polymorphic aposematic moth. *Ecology Letters*, *23*, 1654–1663.

Rowe, C., & Halpin, C. (2013). Why are warning displays multimodal? *Behavioral Ecology and Sociobiology*, *67*, 1425–1439.

Santangelo, V. (2015). Forced to remember: When memory is biased by salient information. *Behavioural Brain Research*, *283*, 1–10.

Stevens, M., & Cuthill, I. C. (2006). Disruptive coloration, crypsis and edge detection in early visual processing. *Proceedings of the Royal Society B: Biological Sciences*, *273*, 2141–2147.

Stevens, M., & Ruxton, G. D. (2012). Linking the evolution and form of warning coloration in nature. *Proceedings of the Royal Society B: Biological Sciences*, *279*, 417–426.

Stoddard, M. C., Kilner, R. M., & Town, C. (2014). Pattern recognition algorithm reveals how birds evolve individual egg pattern signatures. *Nature Communications*, *5*, 10.

Stoddard, M. C., & Osorio, D. (2019). Animal coloration patterns: Linking spatial vision to quantitative analysis. *The American Naturalist*, *193*, 164–186.

Torralba, A., & Oliva, A. (2003). Statistics of natural image categories. *Network: Computation in Neural Systems*, *14*, 391–412.

Troscianko, J., Skelhorn, J., & Stevens, M. (2017). Quantifying camouflage: How to predict detectability from appearance. *BMC Evolutionary Biology*, *17*, 7.

van den Berg, C., Troscianko, J., Endler, J. A., Marshall, N. J., & Cheney, K. L. (2020). Quantitative colour pattern analysis (QCPA): A comprehensive framework for the analysis of colour patterns in nature. *Methods in Ecology and Evolution*, *11*, 316–332.

van Hateren, J. H., & van der Schaaf, A. (1998). Independent component filters of natural images compared with simple cells in primary visual cortex. *Proceedings Biological Sciences*, *265*(1394), 359–366. https://doi.org/10.1098/rspb.1998.0303

Wallace, A. R. (1867). Discussion, March 4th meeting. *Transactions of the Royal Entomological Society of London*, *Series 3*, *5*, lxxx–lxxxi.

Watson, A. B., Barlow, H. B., & Robson, J. G. (1983). What does the eye see best? *Nature*, *302*, 419–422.

Wilby, D., Toomey, M. B., Olsson, P., Frederiksen, R., Cornwall, M. C., Oulton, R., Kelber, A., Corbo, J. C., & Roberts, N. W. (2015). Optics of cone photoreceptors in the chicken (*Gallus gallus domesticus*). *Journal of the Royal Society Interface*, *12*, 20150591.

Wuster, W., Allum, C. S. E., Bjargardottir, I. B., Bailey, K. L., Dawson, K. J., Guenioui, J., Lewis, J., McGurk, J., Moore, A. G., Niskanen, M., & Pollard, C. P. (2004). Do aposematism and Batesian mimicry require bright colours? A test, using European viper markings. *Proceedings of the Royal Society B: Biological Sciences*, *271*, 2495–2499.

SUPPORTING INFORMATION

Additional supporting information can be found online in the Supporting Information section at the end of this article.

Data S1: Supplementary methods on the construction of the University of St Andrews hyperspectral database of Lepidoptera (https://arts.st-andrews.ac.uk/lepidoptera/index.html), links to the lists of species and specimens, supplementary methods on the computations of the main metrics and alternative metrics, supplementary results and illustrations.

How to cite this article: Penacchio, O., Halpin, C. G., Cuthill, I. C., Lovell, P. G., Wheelwright, M., Skelhorn, J., Rowe, C., & Harris, J. M. (2023). A computational neuroscience framework for quantifying warning signals. *Methods in Ecology and Evolution*, *00*, 1–14. https://doi.org/10.1111/2041-210X.14268